

Improvements in DTM generation by using full-waveform airborne laser scanning data

Andreas Ullrich^a, Nikolaus Studnicka^a, Markus Hollaus^b, Christian Briese^b, Wolfgang Wagner^b,
Michael Doneus^c, and Werner Mücke^b

^aRIEGL Laser Measurement Systems GmbH, Austria;

^bChristian Doppler Laboratory “Spatial Data from Laser Scanning and Remote Sensing” at the
Institute of Photogrammetry and Remote Sensing, Vienna University of Technology, Austria;

^cDepartment for Prehistory and Early History of the University of Vienna, Austria;

ABSTRACT

Compared to laser radar systems based on the conventional discrete echo approach, direct detection laser radar systems with echo signal digitization and subsequent full-waveform analysis like the *RIEGL* LMS-Q560 provide valuable additional information on the target’s properties. This additional information can be used in the course of the mandatory processing task of classifying the measurement data into ground returns and non-ground returns. Classification is a prerequisite for generating high-quality digital terrain models (DTMs) based on airborne laser scanning data. We present field data to demonstrate the superiority of full-waveform data over conventional laser data with respect to DTM generation.

Keywords: Laser Radar, LiDAR, Airborne Laser Scanning, Full-Waveform Analysis, Digital Terrain Models

1. INTRODUCTION

The term airborne laser scanning (ALS) describes a nowadays widely used measurement method for acquiring three-dimensional data on a surface. Usually, the ALS system is mounted on an airborne platform and scans the terrain by measuring the travelling time of the pulse from the laser scanner to the Earth’s surface and back. The laser range measurement system is also referred to as LiDAR (light detection and ranging) system. In order to generate highly accurate data in a well-defined global coordinate frame (e.g. WGS84), the orientation and position of the LiDAR system has to be measured with high accuracy and precision. Thus, one of the main components of an ALS system is an integrated inertial measurement unit (IMU) and a global positioning system (GNSS, differential GPS) closely coupled to the scanning LiDAR system, providing the attitude and position of the LiDAR system. With the technological advances of laser scanners, global navigation satellite systems, inertial measurement units, and airplanes, ALS has achieved high economic importance due to its high accuracy capability and has been established as one standard methods for topographic data acquisition. ALS applications range from the generation of digital terrain models to three-dimensional city models, and to vegetation (e.g. forest parameters) or corridor (e.g. power lines) mapping.

LiDAR systems relying on the pulsed time-of-flight principle are capable of providing more than one range reading per laser pulse if several objects interfere with the laser beam. Conventional discrete echo ALS systems record at least the first or the last detectable echo. However, most of the current systems allow detecting the first and the last echo while only some systems deliver up to four echoes from multiple targets illuminated by a single laser pulse. The output of such systems is typically a set of three-dimensional coordinates and a so-called intensity information per detected echo. However, due to unknown characteristics of the target (size, reflectance, laser radar cross-

section), the intensity values are rarely used in commercial applications to infer physical characteristics of the backscattering target. In contrast to these discrete echo ALS systems, systems based on echo signal digitization and subsequent full-waveform analysis offer more information per laser pulse and are deemed to be able to infer valuable characteristics of the interfering targets.

In almost all applications the processing of ALS data, especially for the generation of digital terrain models (DTM), a classification into terrain and off-terrain points is required. Usually, this is achieved by using various filtering techniques [1] that classify the point cloud into terrain and off-terrain points just based on the geometric and topologic relationship of the 3D data [2]. However, if there are several spatially distributed targets within a laser path, as it is typically the case in forested areas, only a fraction of the laser energy is scattered back by the top of the canopy, while the remaining energy can penetrate through small gaps and may be reflected by branches, bushes or finally by the terrain. In this case the returning signal is a superposition of single echoes from different scatterers. A successful separation of two neighboring targets along the pulse path requires a minimum distance, corresponding to the so-called range resolution. The capability of discrimination between near by targets depends on the system parameters, e.g., pulse width, system bandwidth, but also on the signal detection and signal processing schemes implemented in the LiDAR system.

As pointed out in [3] and [4] the full-waveform data has in comparison to conventional discrete ALS data the advantage that the users can apply their own echo detection method in post-processing. This makes the ranging process more transparent and robust and may lead to a higher accuracy of the derived distances. In addition to the improved range measurements, full-waveform data allows the extraction of physical observables of the reflecting surface elements. Using a Gaussian decomposition approach [5] the range, the echo width and the amplitude can be determined for each detected echo and finally, the backscatter cross-section can be computed. First studies have shown the high potential of these additional physical quantities for advanced object classification [6, 7] which can be used for an improved classification of the ALS points into terrain and off-terrain points leading to DTMs with higher qualities [8, 9].

The subsequent sections provide a short description of the echo-digitizing ALS system (*RIEGL LMS-Q560*), the full-waveform analysis based on Gaussian decomposition, and the generation of the digital terrain model making use of additional information from full-waveform analysis in order to pre-classify points and to generate a high quality DTM. The improvements with respect to conventional data and conventional processing are demonstrated by example data.

2. FULL-WAVEFORM SYSTEM

Figure 1 illustrates the process of echo signal digitization. The top most line depicts the analog echo signals: the first (left most) pulse relates to the laser transmitter pulse, and the following pulses correspond to the reflections by objects within the laser beam. The temporal distance of the signals with respect to the transmitter pulse signal corresponds to the range. The last signal relates to the most distant target giving rise to a detectable echo signal. This analog echo signal is sampled at constant time intervals (middle line) and is subsequently analog-to-digital (AD) converted, resulting in a digital data stream (bottom line of the acquisition section). Commonly the laser pulse repetition rate is chosen to match the range gate length, i.e., the maximum unambiguous detectable range. In this case, the data rate generated by echo digitization is huge, typically 2 giga samples per second. In order to achieve reasonable data rates, the amount of data is reduced by means of thresholding. Thus only the sample data containing information on detected targets is transmitted to a data recorder for further offline analysis.

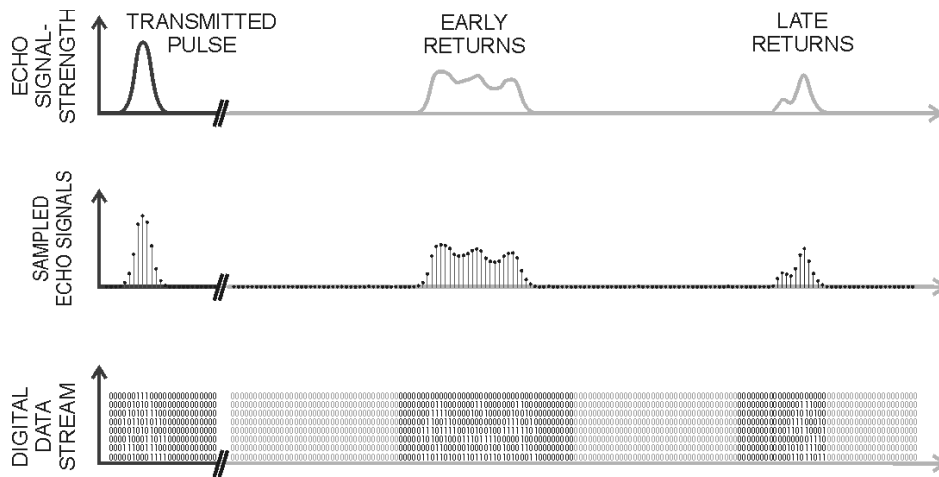


Figure 1. Principle of echo digitization.

In a post-processing step the signal is perfectly reconstructed offline and is analyzed in detail by applying appropriate algorithms, e.g., by fitting corresponding replica of the transmitted waveform to the echo signal such as Gaussian pulses as discussed below. The temporal position of the target with respect to the transmitted pulse gives the absolute target range. The temporal distance between echo pulses gives highly accurate range information on the distance between objects. The width information of the echo pulse provides information on the surface roughness, the slope of the target, or the depth of a volumetric target, e.g., a layer of fog. The amplitude of the echo signal provides information on the target's laser radar cross-section or directly on the target's reflectance in case of targets larger than the laser footprint.

For surveying applications the major benefits of echo digitization in combination with off-line full-waveform analysis are: access to an unlimited number of targets per laser measurement, an excellent multi-pulse resolution, information on surface roughness and/or surface slope, and a profound estimation of the laser radar's cross-section of the targets detected.

The commercially available laser radar system designed for airborne laser scanning applications employing echo digitization, the *RIEGL LMS-Q560* [10] and the data recorder *RIEGL DR560 / DR560-RD*, is shown in Figure 2.

The laser instrument scans its measurement beam linearly of a configurable wide field-of-view. Combining the laser scanner with IMU/GPS (inertial measurement system/ global positioning system) results in a state-of-the-art airborne LiDAR mapping system. The high measurement rate and the high line scan rate provide a superior density of measurements on terrain with an even distribution of laser footprints on the terrain. The instrument is extremely rugged, compact, and lightweight enough to be installed in small single-engine planes, helicopters, or even ultra-light planes. Table 1 summarizes the key specification of the laser scanner.

For airborne laser scanning the system has to be complemented by at least an INS/GPS subsystem, mechanically firmly coupled to the laser scanner, and a computer subsystem to control the system and to store the raw data for further processing. In many cases a mid-format digital camera provides additional data for, e.g., generation of orthophotos. As an example, Figure 3 shows a commercial turn-key ALS system based on two *RIEGL LMS-Q560* and an aircraft from Diamond Airborne Sensing, the multi-purpose platform DA42 MPP. The system parameters are summarized in Table 2.

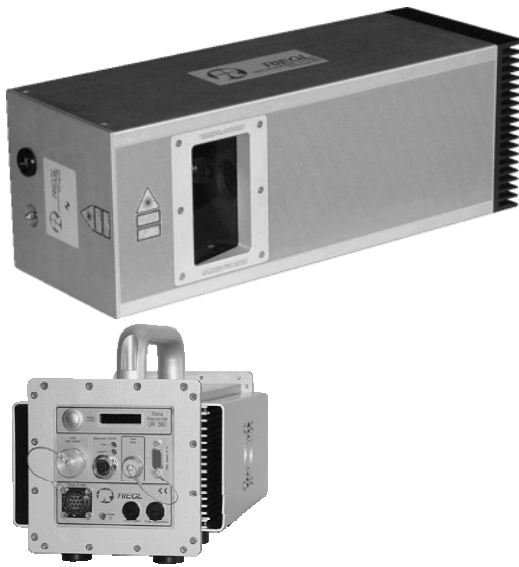


Figure 2. RIEGL LMS-Q560 (top) and RIEGL DR560 (bottom).

Parameter	Value
Measurement range	30 m - 1800 m @ target reflectivity of 60% 30 m - 1200 m @ target reflectivity of 20%
Ranging accuracy	20 mm
multi-target resolution	down to 0.5 m
Measurement rate	240 000 measurements / s (burst rate) up to 160 000 measurements/ s (average)
Scan range	45° (up to 60°)
Scan speed	up to 160 lines / sec
Synchronization	GPS PPS (pulse per second) & serial interface
Time stamping	resolution 1 μ s, unambiguous range > 1 week
Size / weight	560 x 200 x 217 mm / 20 kg
Laser safety	laser class 1 / wavelength near infrared

Table 1. Key specifications of *RIEGL LMS-Q560*.



Figure 3: ALS system based on two RIEGL LMS-Q560 and Diamond Airborne Sensing DA42 MPP.

aircraft	Diamond DA42 MPP	
air speed	40 m/s -80 m/s	
laser scanner	<i>RIEGL LMS-Q560</i> , full-waveform capabilities	
spatial density, 45 m/s (2 laser scanner)	AGL = 450 m	AGL = 800 m
@ 2 x 100 kHz PRR	6 meas / m ²	3.4 meas / m ²
@ 2 x 240 kHz PRR	14 meas / m ²	--
storage capacity	> 8 hours of full-waveform data recording	
ranging accuracy	2 cm	
geo-referenced accuracy	10 cm experimental data: less than 3 cm (1s) wrt reference objects, after post-processing with flight line adjustment	
approvals	certification category EASA part 23 (Europe), FAR23 (USA) , enables worldwide operation	

Table 2: System parameters of the *RIEGL/Diamond ALS* system.

3. DATA PROCESSING

3.1 Test site and data

The test site is located within the Leitha mountain range, 50 km southeast of Vienna. The central area of the Leitha mountain range is covered by forests, whereas the main tree species are oak and beech with a varying range of understory. In the boarder regions agricultural land and few buildings can be found. The entire area is covered with full-waveform ALS data acquired with a *RIEGL* Airborne Laser Scanner LMS-Q560, operated by the company Milan Flug GmbH. The data acquisition took place between March 28th and April 12th, 2007. The average flying altitude was 600 m above ground, resulting in an average laser beam footprint size of 30 cm on ground. The point density (i.e. last-echoes) ranges between 5 and 7 points per m². The technical parameters of the LMS-Q560 are summarized in Table 1.

3.2 Full-waveform data processing

As reported by [5] the system waveform of the *RIEGL* LMS-Q560 is well described by a Gaussian function. Consequently, the received backscattered waveform is a result of a convolution of the system waveform and the differential cross-section of the illuminated object surface. A complex waveform caused by several backscattering targets can be modeled by the following formula:

$$P_r(t) = \sum_{i=1}^N \hat{P}_i e^{-\frac{(t-t_i)^2}{2s_{p,i}^2}} \quad (1)$$

where $P_r(t)$ is the received power, t_i is the round trip-time of target i , \hat{P}_i is the amplitude of target i , $s_{p,i}$ is the standard deviation of the echo pulse from target i , and N is the number of targets within the path of the emitted laser pulse [5]. Based on this Gaussian decomposition the range to each detectable echo, the amplitude, and the echo width is obtained. Due to the short laser pulse duration of the LMS-Q560 ($\tau = 4$ ns) scattering targets, which are separated by a minimum distance of 0.6 m can be differentiated. As shown in [5] the radar equation can be adapted for converting the received power P_r into the backscatter cross-section σ_i , which is a calibrated physical quantity. It is the effective area of collision of the laser beam and the target, taking into account the directionality and strength of reflection. Thus, it describes how much energy of an incoming electromagnetic wave is scattered back by the target. For each detected echo σ_i can be calculated using the following equation:

$$\sigma_i = C_{cal} R_i^4 \hat{P}_i s_{p,i} \quad (2)$$

where C_{cal} is the calibration constant and R_i the range of target i . For the calibration of the data asphalt roads are used as reference targets. It is assumed that the average reflectivity of asphalt roads is 0.2 and that they behave like an ideal Lambertian scatterer [5]. Furthermore, it is assumed that the power losses in the instrument and in the atmosphere are consistent within the used data. According to the findings of [6] σ_i values of individual echoes depend strongly on the number of backscattering echoes within the laser footprint. Thus, the total backscatter cross section σ_t , which represents the entire backscattered energy for each emitted laser pulse is calculated by the following formula:

$$\sigma_t = \sum_{i=1}^N \sigma_i \quad (3)$$

The derived quantities are illustrated in Figure 4. In Figure 4b the amplitudes are shown, which depend on the reflectivity of the target, on the number of echoes per laser shot and on the range between the laser scanner and the target. Figure 4d shows the total backscatter cross-section, which

is independent of the range and of the number of echoes per laser shot. It can be seen that laser shots, which contain also an echo backscattered from terrain are characterized by higher σ_t than those laser shots which contain only echoes backscattered from off-terrain (i.e. vegetation) points. The echo width represents the range distribution of all individual scatterers contributing to one echo. Consequently the echo width is quite narrow in open terrain areas and increases for echoes backscattered from rough surfaces (e.g. canopy, bushes, grasses, etc.). As shown in Figure 4c areas with smooth and rough surfaces can clearly be differentiated within the echo width image. Even for fields covered with grass or cereals (vegetation height approx. 30 cm) a clear widening of the echo width occur as can be seen in the two fields shown in the upper and lower right corner of Figure 4c.

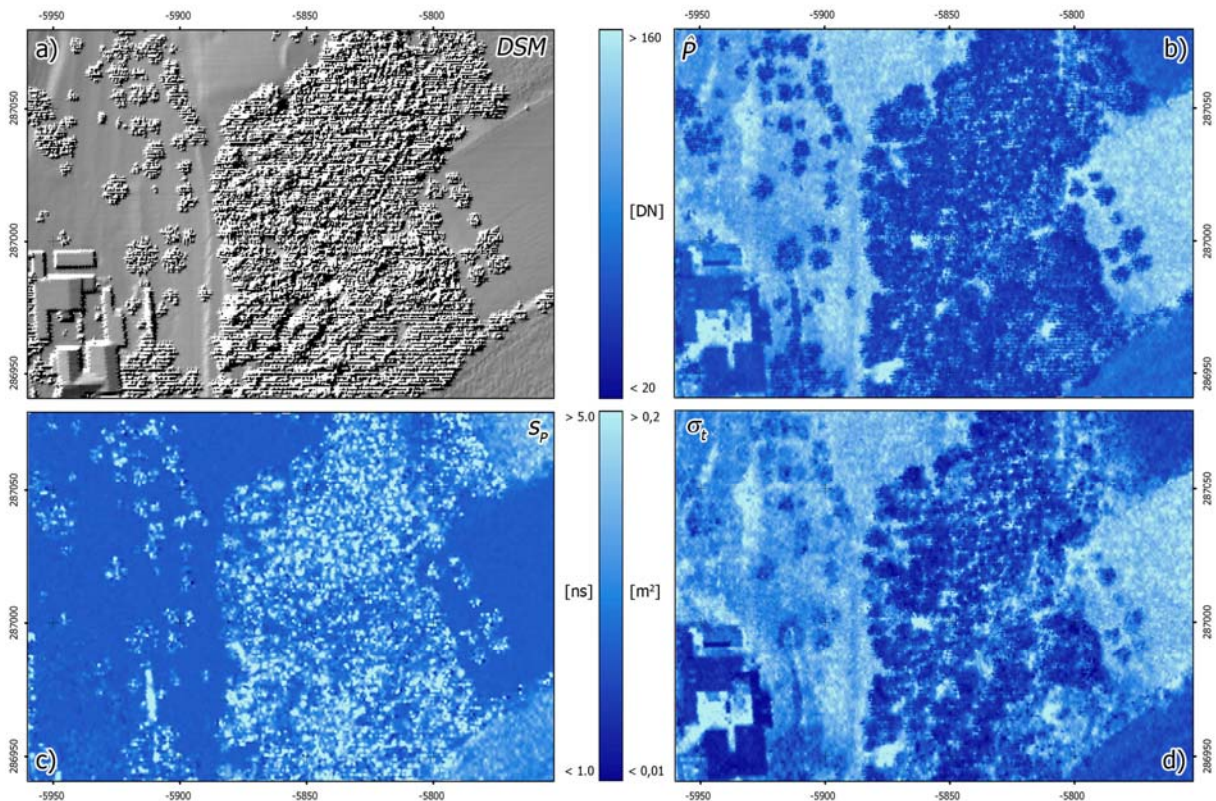


Figure 4. Physical quantities derived from full-waveform ALS data. Shown are (a) the shaded digital surface model, (b) the amplitudes, (c) the echo widths, and (d) the total backscatter cross section projected into the position of the last echo.

4. IMPROVED DTM GENERATION

The generation of DTMs from ALS data requires a filtering (classification) of the point cloud into terrain and off-terrain points. Many different filtering algorithms [1] were developed in the past. All these approaches have in common that they rely only upon geometric criteria (e.g. height relation to neighboring points) for the elimination of off-terrain points. For the current analyses the hierarchic robust filtering technique is used for the generation of the DTM. The robust filtering procedure was introduced in [11] and basically rests upon the assumption that low lying, clustered point clouds are more likely to belong to the terrain compared to higher lying points. Its extension into a hierarchic framework is described in detail in [12]. The hierarchic robust filtering procedure is implemented into the software package SCOP++¹.

¹ <http://www.ipf.tuwien.ac.at/products>; <http://www.inpho.de>

To consider the information derived from full-waveform ALS data [6, 13, 14] have used the echo width to pre-classify the last-echoes into terrain and off-terrain points. In addition to the echo width the total backscatter cross-section can be used for the pre-classification of the last echoes. In Figure 5 pre-classified off-terrain points are shown, whereas simple thresholds for the echo width and the total backscatter cross-section were applied. Finally, the pre-classified terrain points can be used for the DTM modeling.

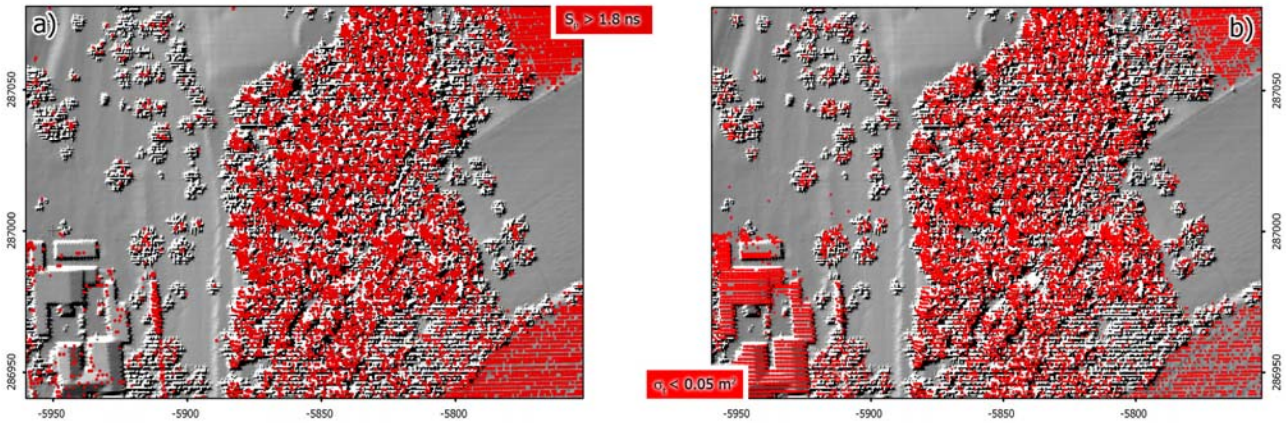


Figure 5. Digital surface models overlain with pre-classified off-terrain points. For the classification a threshold was applied for (a) the echo width and (b) total backscatter cross-section.

However, this approach has to be used with care as it cannot recover inevitable pre-classification errors. Therefore, [9] have expanded the hierarchic robust filtering approach to the usage of individual a-priori weights of all last echoes. Terrain points are typically characterized by small echo widths and off-terrain points by higher ones as shown in Figure 4c. Thus, small echo widths are assigned to high a-priori weights and vice versa. Instead of the echo width also the total backscatter cross-section can be used for the estimation of the a-priori weights. Therefore, the geometric and the physical properties of the detected echoes can be included for the robust surface estimation. Figure 6b illustrates the DTM improvements by considering the echo width derived from full-waveform ALS data. Especially, for areas covered by low vegetation the applied individual weights leads to a more reliable DTM.

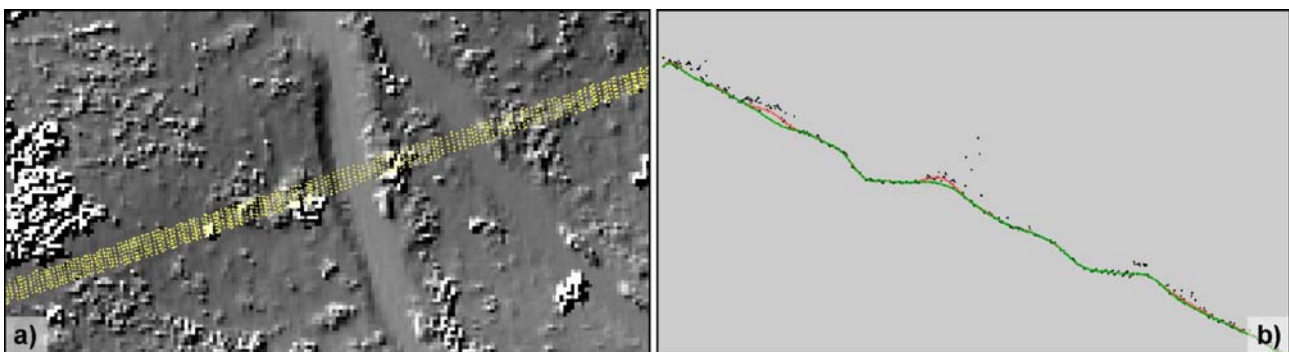


Figure 6. a) Digital surface model overlain with the last echoes shown in b. b) DTMs generated by robust estimation with (green line) and without (red line) individual a-priori weights. The individual weights are based on the echo width. The last echo points are shown as black dots.

5. SUMMARY AND CONCLUSION

This paper gives an overview on an echo digitizing airborne laser scanning system and the full-waveform analysis, and demonstrates the utilization of full-waveform data for the generation of DTMs with improved accuracy. The improvement is based on additionally available observations for each target echo, i.e., echo width and an estimate for the total backscatter cross-section for each laser shot. For the hierarchic robust filtering approach individual a-priori weights were used, which were derived from the echo widths. Finally, it could be shown that the DTM generated from the last echoes including the echo width achieve a higher quality than those generated from last echo points without the echo width. Within the forested area small artifacts caused by bushes, brushwood, or piles of twigs could successfully be removed, which would not be possible in an automatic processing chain if only the three-dimensional coordinates were used. Further improvements of the DTM could also be reached within agricultural land covered by high, dense grass or cereals. The advantage of full-waveform laser scanning opens therefore new possibilities for, e.g., archeological prospection below forest cover by increasing the terrain model accuracy.

ACKNOWLEDGEMENTS

The ALS data are provided by Michael Doneus, Department for Prehistory and Early History of the University of Vienna, from a project funded by the Austrian Science Fund (FWF - project no. P18674-G02). Finally, we would like to thank Helmut Kager from the Institute of Photogrammetry and Remote Sensing (I.P.F.), Technical University of Vienna and Thomas Melzer from the Christian Doppler Laboratory for Spatial Data from Laser Scanning and Remote Sensing at the I.P.F. for their support to process the data.

REFERENCES

1. Sithole, G.; Vosselman, G. Experimental comparison of filter algorithms for bare-Earth extraction from airborne laser scanning point clouds, *ISPRS Journal of Photogrammetry & Remote Sensing*. **2004**, 59(1-2), 85-101.
2. Pfeifer, N.; Gorte, B.; Elberink, S. O. Influences of Vegetation on Laser Altimetry - Analysis and Correction Approaches, *Proceedings of ISPRS workshop "Laser-Scanners for Forest and Landscape Assessment"*, Freiburg, Germany, **2004**, XXXVI, Part 8/W2, 283-287.
3. Wagner, W.; Ullrich, A.; Melzer, T.; Briese, C.; Kraus, K. From single-pulse to full-waveform airborne laser scanners: Potential and practical challenges, *Proceedings of International Society for Photogrammetry and Remote Sensing XXth Congress, Vol XXXV, Part B/3, 12-23 July 2004, Commission 3*, Istanbul, Turkey, **2004**, Vol. XXXV, part B3, 6.
4. Ullrich, A.; Reichert, R. High resolution laser scanner with waveform digitization for subsequent full waveform analysis, *Proceedings of Proceedings of SPIE - Laser Radar Technology and Applications X*, **2005**, 5791, 82-88.
5. Wagner, W.; Ullrich, A.; Ducic, V.; Melzer, T.; Studnicka, N. Gaussian decomposition and calibration of a novel small-footprint full-waveform digitising airborne laser scanner, *ISPRS Journal of Photogrammetry & Remote Sensing*. **2006**, 60(2), 100-112.
6. Wagner, W.; Hollaus, M.; Briese, C.; Ducic, V. 3D vegetation mapping using small-footprint full-waveform airborne laser scanners, *International Journal of Remote Sensing*. **2007**, in press.

7. Hug, C.; Ullrich, A.; Grimm, A. Litemapper-5600 - A Waveform-Digitizing LiDAR Terrain and Vegetation Mapping System, *International Archives of Photogrammetry, Remote Sensing and Spatial Information Sciences*. **2004**, XXXVI, PART 8/W2.
8. Doneus, M.; Briese, C. Digital terrain modelling for archaeological interpretation within forested areas using full-waveform laserscanning, *CIPA International Workshop, Nicosia, Cyprus; 10-30-2006 - 11-04-2006*; in: "VAST 2006", M. Ioannides, D. Arnold, F Niccolucci, K. Mania (ed.); *The 7th International Symposium on Virtual Reality, Archaeology and Cultural Heritage VAST (2006)*. **2006**, 155 - 162.
9. Mandlburger, G.; Briese, C.; Pfeifer, N. Progress in LiDAR sensor technology - chance and challenge for DTM generation and data administration, *Proceedings of the 51th Photogrammetric Week, 09-03-2007 - 09-07-2007*, Stuttgart, **2007**, 159-169.
10. RIEGL Laser Measurement Systems GmbH. Technical data at www.riegl.com, 2007.
11. Kraus, K.; Pfeifer, N. Determination of terrain models in wooded areas with airborne laser scanner data, *ISPRS Journal of Photogrammetry & Remote Sensing*. **1998**, 53(4), 193-203.
12. Briese, C.; Pfeifer, N.; Dorninger, P. Applications of the Robust Interpolation for DTM Determination, *International Archives of Photogrammetry and Remote Sensing*. **2002**, XXXIV (Part 3A), 55-61.
13. Doneus, M.; Briese, C. Full-waveform airborne laser scanning as a tool for archaeological reconnaissance, In: "From Space to Place". *Proceedings of the 2nd International Conference on Remote Sensing in Archaeology, BAR International Series, 1568*. **2006**, 99-105.
14. Ullrich, A.; Hollaus, M.; Briese, C.; Wagner, W.; Doneus, M. Utilization of full-waveform data in airborne laser scanning applications, *Proceedings of Conference Proceedings of the SPIE Defense and Security Symposium, Volume 6550, 9 - 13 April 2007*, Orlando, Florida USA, **2007**, pp. 12.